

## ADVANCED UAV PATH PLANNING AND CLUSTERING TECHNIQUES FOR 3D RECONSTRUCTION OF POST-EARTHQUAKE ARCHITECTURES

JIANFENG CHE<sup>1,2</sup>, SWEE KING PHANG<sup>1,\*</sup>, LIN GE<sup>1</sup>

<sup>1</sup>School of Engineering, Taylor's University, Taylor's Lakeside Campus,  
No. 1 Jalan Taylor's, 47500, Subang Jaya, Selangor DE, Malaysia

<sup>2</sup>Department of Intelligent Manufacturing,  
Chengde College of Applied Technology, Chengde, China

\*Corresponding Author: [sweeking.phang@taylors.edu.my](mailto:sweeking.phang@taylors.edu.my)

### Abstract

This research provides an exhaustive examination of the pivotal role that three-dimensional (3D) reconstruction techniques play in the post-seismic assessment of architectural structures, with a pronounced emphasis on the deployment of Unmanned Aerial Vehicles (UAVs). Given the profound ramifications of seismic events on urban infrastructures, the study underscores the imperative of conducting timely and meticulous evaluations of the affected edifices. The paper commences by undertaking a 3D modelling of the architectural ensemble, strategically positioning cameras around the target structures to capture previously uncharted points. Subsequently, two sophisticated clustering algorithms, namely spectral clustering and Fuzzy K-means, are employed to cluster these positional points. These clustered points are then judiciously allocated to a fleet of four UAVs for optimal coverage. The research introduces the F-RRT\* algorithm, an augmented version of the conventional RRT\* algorithm tailored for path planning. This enhancement is spotlighted for its superior convergence rate and its ability to generate more streamlined and efficient trajectories. In summation, this comprehensive investigation furnishes invaluable insights and avant-garde technical methodologies for post-disaster architectural evaluations, championing the advancement of UAV-centric 3D reconstruction endeavours.

Keywords: 3D Reconstruction, Intelligent system, Path planning, Post-disaster, UAV.

## 1. Introduction

The perpetual movement of tectonic plates on the Earth has rendered earthquakes a significant natural peril that can potentially affect all regions of the globe [1]. In recent times, a series of devastating earthquakes have resulted in significant human and infrastructural losses. Among the most affected infrastructures are buildings, which are pivotal in human life as primary residences and workspaces. Their vulnerability during seismic events often results in substantial damage, jeopardizing their structural integrity and safety [2]. Post-disaster, there is an urgent need for a swift and precise assessment of these structures. Such evaluations are not just pivotal for human safety but also set the stage for informed decisions in the subsequent recovery and rebuilding phases. 3D building reconstruction emerges as a potent tool, facilitating comprehensive visual inspections of damaged buildings across varied angles and dimensions. By generating detailed 3D building representations and providing essential data that aids in the restoration process [3].

In the evolution of 3D reconstruction technology, numerous methods and strategies have been proposed and extensively researched. For instance, laser scanning technology, despite its unparalleled measurement accuracy, is limited in its widespread adoption for large-scale and remote applications due to high requirements in equipment investment and operational complexity [4]. Stereophotography, as an economically efficient approach, still possesses certain advantages in certain application scenarios, although it may encounter difficulties in handling complex surfaces and textures [5].

Structured light scanning technology exhibits outstanding performance in indoor environments, but its application in outdoor settings is hindered by interference from natural light, thus limiting its scope of use [6]. Given the limitations of the aforementioned techniques, unmanned aerial vehicles (UAVs) offer a promising alternative for 3D building reconstruction [7]. They can rapidly cover large areas, particularly in terrains that are complex or difficult to access. By incorporating high-resolution imaging technology, UAVs can capture rich details, providing high-quality data input for subsequent 3D modelling [8]. Furthermore, their unique manoeuvrability allows for capturing images from multiple angles, further enhancing the accuracy and completeness of the 3D model [9].

In the realm of 3D reconstruction of buildings using unmanned aerial vehicles (UAVs), path planning holds paramount importance. Proper path planning ensures the safety of the UAV during flight by avoiding collisions with other objects, while also ensuring efficient and high-quality image capture [10]. Optimizing the flight path guarantees the capture of images from the optimal angles and positions, thereby enhancing the accuracy and completeness of the 3D model. Furthermore, effective path planning conserves the UAV's battery and extends its flight time, thereby improving overall operational efficiency.

In recent years, numerous scholars have delved deep into the study of UAV path planning. Yang et al. have developed an unmanned aerial vehicle (UAV) path planning method aimed at ensuring the desired image overlap and optimizing the flight route during the application of UAVs for digital terrain model (DTM) reconstruction [11]. Qi Kuang et al. has proposed an UAV real-time path-planning method for autonomous urban scene reconstruction [12]. Song et al. proposed a novel view path planning method based on an online Multi-View Stereo (MVS) system [13]. This method aims to incrementally construct a target three-

dimensional (3D) model in real time. Ryosuke Nagasawa et al. has proposed a multi-UAV coverage path planning method for the three-dimensional reconstruction of post-disaster damaged buildings [14]. This method has been implemented in the multi-agent modelling environment NetLogo3D and tested in the virtual construction environment of Unity3D.

Despite many path planning algorithms being proposed, the challenge of selecting and optimizing algorithms suitable for the 3D reconstruction of post-disaster buildings remains [15]. Scholars have conducted research in this area. Particularly in complex urban environments, where there are numerous damaged buildings, a single UAV is insufficient for the reconstruction task, and multiple UAVs are required for task allocation. This poses a great challenge to path planning [16].

Clustering methods also play a critical role in UAV-based 3D building reconstruction. Although various clustering methods, such as K-MEAN and spectral clustering, have been proposed and applied, the selection and optimization of the most suitable clustering method for this application scenario is still an open research question [17]. This is especially true when considering the 3D reconstruction task with multiple UAVs, where ensuring effective collaboration among UAVs and addressing task allocation and energy management are important research directions.

This study aims to explore new methods and strategies for path planning of drones in 3D building reconstruction. Modelling of disaster-stricken areas and generating 3D building models are conducted. In addition, shooting positions are set around each target building. A novel clustering method is introduced to allocate tasks more effectively and optimize flight paths. Finally, the path planning problem is transformed into the traveling salesman problem, and a path planning algorithm is designed to achieve optimal flight costs. This research will provide more advanced and practical technical support for the rapid and accurate assessment of post-disaster buildings. Through these innovative approaches, it is expected to make meaningful contributions to the field of drone-based 3D building reconstruction.

## 2. Methodology

In this section, a systematic strategy for post-disaster structural reconstruction using UAVs is delineated in Fig. 1. 3D models for 25 structures are constructed, with 13 designated as primary targets for reconstruction. Precise determination of camera angles and positions is imperative for capturing accurate and comprehensive 3D representations. Utilizing clustering techniques ensures efficient distribution of camera positions across multiple drones, guaranteeing coverage of distinct, non-overlapping areas.

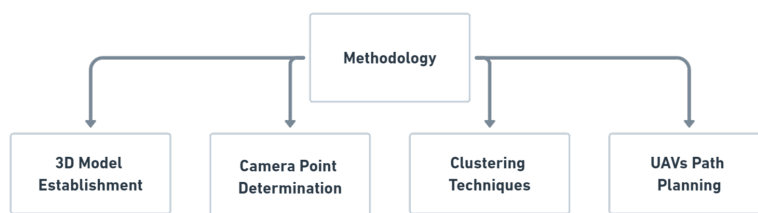


**Fig. 1. Workflow and scope of this methodology.**

The Robust and Sparse Fuzzy K-Means Clustering Algorithm approach is examined in depth and contrasted with spectral clustering to discern relative merits. Central to the research is the development of drone flight paths. Given constraints such as battery duration and flight range, F-RRT\* path planning algorithms are selected and augmented with optimization methods to ensure optimal flight performance and safety.

The primary objective of this model's construction lies in establishing a foundational framework for subsequent camera positioning and path planning, ensuring comprehensive observation and analysis of architectural structures [18]. Initialization of the model involves setting a deterministic seed for the random number generator, guaranteeing reproducibility across various iterations. Parameters including number of buildings, dimensions, spacing, and potential height variations were defined [19]. Buildings are characterized by a width of 25 units, a depth of 30 units, and a height, randomly ascertained, ranging between 40 and 150 units. Emulating the inherent unpredictability of urban sprawl, building positions, originally grid-based, undergo randomization. A dichromatic scheme differentiates the structures: deep blue signifies target buildings central to this investigation, whereas red demarcates ancillary structures.

Conclusively, this 3D modelling offers an invaluable instrument for stakeholders in urban planning and architectural design, presenting a holistic architectural layout via a 3D visualization crafted using MATLAB's fill3 function. This visual representation is denoted as 3D Representation of Buildings in Fig. 2.

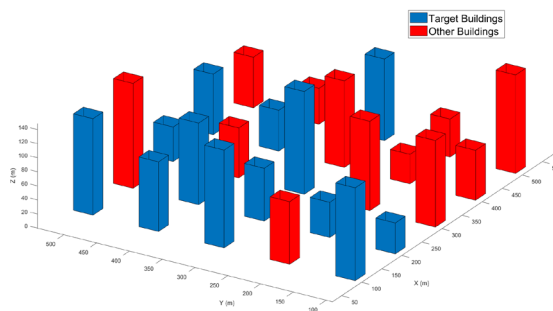


Fig. 2. 3D representation of buildings.

### 2.1. Arrangement of camera shooting points

In the context of 3D architectural reconstruction, the strategic selection of camera shooting positions is of paramount importance [20]. To ensure the accuracy and completeness of the 3D model, this study adopts a comprehensive strategy for choosing camera shooting points [21]. Firstly, considering the scenario of multiple cooperative unmanned aerial vehicles (UAVs), a planning adjustment mechanism is introduced to analyse the flight trajectories of each UAV and the estimated image acquisition time, ensuring a safe distance between UAVs to avoid collisions and image overlap. Secondly, a series of fundamental parameters are defined, including the flight speed of the UAVs, the field of view angle of the camera, and the expected image overlap rate, which serve as the basis for subsequent selection of shooting points.

Furthermore, to ensure the continuity and overlap of images, the camera footprint for each shooting position is calculated based on the camera's focal length, sensor size, and predetermined flight altitude. Lastly, in order to further optimize the selection of shooting points, an overlap measurement mechanism is introduced, which compares the overlapping areas between consecutive images to ensure that each image provides sufficient information for the 3D reconstruction. The following Table 1 presents the camera shooting point-related information.

**Table 1. Camera shooting point-related parameter.**

Parameter	Description
Planning Adjust	Consideration of the distance between drones to avoid flying too close
Basic Parameters	Determined by drone speed, camera field of view, and expected image overlap
Camera Footprint	Based on camera focal length, sensor size, and flight altitude
Overlap Measure	Optimization of shooting point selection by comparing overlap areas of consecutive images

## 2.2. Two types of clustering algorithms

In this study, two clustering algorithms were employed to analyse the data. Firstly, the spectral clustering algorithm was introduced as a reference benchmark. Spectral clustering, as a graph-based method, possesses certain advantages in handling complex data structures. However, despite its impressive performance in certain application scenarios, it does not always meet all clustering requirements. Therefore, in order to delve deeper into and address the specific issues in our research, Fuzzy K-Means was selected as the primary clustering algorithm in this paper. Fuzzy K-Means is capable of providing a membership degree for each data point, rather than a fixed class label, making it more flexible and robust in handling fuzziness and uncertainty. Through this approach, our aim is to ensure that the chosen clustering method maximally meets the research needs and provides a reliable foundation for subsequent analysis.

### 2.2.1. Spectral clustering algorithm

The spectral clustering technique is rooted in graph theory. It envisions data points as graph nodes and builds the graph by gauging the similarity between these nodes [22]. Within this graph, edges connecting similar data points carry higher weights, whereas those linking dissimilar points have reduced weights or none at all. The goal of spectral clustering is to group these nodes so that nodes within a group share high similarity, and those across different groups have low similarity. The underlying mathematical representation of spectral clustering is given by the subsequent formula.

Compute the similarity matrix: For each pair of data points  $x_i$  and  $x_j$  in a dataset, the similarity between them is calculated, usually using a Gaussian kernel function or other kernel function.

$$S_{ij} = \exp\left(-\frac{\|x_i - x_j\|^2}{2\sigma^2}\right) \quad (1)$$

where  $\sigma$  is the width parameter of the Gaussian kernel.

Calculation degree matrix  $D$  is a diagonal matrix, where each diagonal element  $d_{ii}$  is the degree of node  $i$ , the sum of the weights of all edges connected to node  $i$ .

$$d_{ii} = \sum_{j=1}^n S_{ij} \quad (2)$$

Compute the Laplace matrix

$$L = D - S \quad (3)$$

Standardized Laplace matrix

$$L_{sym} = D^{-1/2} L D^{-1/2} \quad (4)$$

Calculation the eigenvectors corresponding to the smallest  $k$  non-zero eigenvalues of  $L$  and use these eigenvectors for  $k$ -means clustering.

### 2.2.2. Robust and sparse fuzzy K-means clustering algorithm

The conventional fuzzy K-means clustering algorithm may suffer from the influence of noise and outliers, resulting in a decrease in the accuracy of the clustering results [23]. To address this issue, researchers have proposed the robustness and sparsity-based fuzzy K-means clustering algorithm. This algorithm combines the advantages of sparsity and robustness, enhancing its stability and accuracy when dealing with noise and outliers.

The Robust and Sparse Fuzzy K-Means Clustering algorithm focuses primarily on three core formulas, which collectively define how to compute the membership degrees of data points, how to update cluster centres, and how to optimize the weights of data points [24].

Affiliation matrix  $U = [u_{ij}]$ :

$$u_{ij} = \frac{1}{\sum_{k=1}^c \left( \frac{\|x_i - v_j\|^2}{\|x_i - v_k\|^2} \right)^{\frac{2}{m-1}}} \quad (5)$$

where  $u_{ij}$  denotes the degree of affiliation of data point  $x_i$  belonging to cluster  $j$ ,  $v_j$  is the center of cluster  $j$ ,  $c$  is the number of clusters and  $m$  is the ambiguity parameter (usually greater than 1).

Cluster centre  $v_j$  is updated:

$$v_j = \frac{\sum_{i=1}^n w_i u_{ij}^m x_i}{\sum_{i=1}^n w_i u_{ij}^m} \quad (6)$$

where  $w_i$  is the weight of data point  $x_i$ , which can be optimized by sparsity constraints and a robustness loss function.

The update of the weight matrix  $w$  can be solved by the following optimization problem:

$$\min_w \sum_{i=1}^n \sum_{j=1}^c u_{ij}^m l(x_i, v_j, w_i) + \lambda \|w_i\|_1 \quad (7)$$

where  $l$  is the robustness loss function, the  $\lambda$  is the regularization parameter for the sparsity constraint. The comparison of the steps for the two algorithms is illustrated in Table 2.

**Table 2. Comparison of clustering methods: spectral clustering vs. robust and sparse fuzzy K-means clustering.**

Steps	Spectral clustering	Robust and sparse fuzzy K-means clustering
1	Construct the similarity matrix S using the Gaussian kernel function.	Determine the number of clusters c and initialize the cluster centres.
2	Compute the degree matrix D.	Calculate the membership matrix U based on the initial cluster centres.
3	Formulate the Laplacian matrix L.	Compute the objective function $J_m$ using U, cluster centers, and data points.
4	Calculate the eigenvectors and eigenvalues of L.	Update the cluster centres based on U.
5	Select k smallest eigenvalues and their corresponding eigenvectors to form matrix X.	Update U based on the new cluster centres.
6	Use K-means to cluster the rows of X.	Calculate the sparsity-inducing regularization term and incorporate it into $J_m$ .
7	Obtain the final cluster assignments.	Iterate steps 3-6 until $J_m$ converges or a predefined number of iterations is reached.
8	-	Obtain the final cluster assignments based on U.

### 2.3. Path planning algorithm

Given the consideration of flight costs associated with UAVs, it is imperative to identify a flight path with the lowest possible expenses. Hence, this paper employs the F-RRT\* algorithm as the chosen method for path planning.

F-RRT\* is an improved version of the RRT\* (Rapidly-exploring Random Trees Star) algorithm. The main idea of F-RRT\* is that in each iteration, instead of just considering the nearest node to expand, a set of nearest-neighbouring nodes are considered and the best of them are selected for expansion. In this way, the algorithm can explore the configuration space faster and find high-quality paths earlier.

Compared to the standard RRT\* algorithm, F-RRT\* exhibits a faster convergence rate. This indicates that it can find optimal or near-optimal paths in fewer iterations. Additionally, the paths generated by F-RRT\* tend to be smoother and more direct, making it particularly suitable for applications where efficiency and safety are of paramount importance, such as unmanned aerial vehicle flight planning. The specific flow of the F-RRT\* algorithm is shown in Table 3.

**Table 3. Specific description of each step of the F-RRT\* algorithm.**

Step	Process	Description
1	Initialization	Start with an initial node $q_{start}$ , and define the goal node $q_{goal}$ .
2	Sampling	In each iteration, randomly sample a point $q_{rand}$ in the search space.
3	Nearest Node	Find the node $q_{nearest}$ in the tree that is closest to $q_{rand}$ .
4	Steering	Generate a new node $q_{new}$ by moving from $q_{nearest}$ towards $q_{rand}$ but within a maximum distance, Delta q.
5	Obstacle Check	Ensure the path segment between $q_{nearest}$ and $q_{new}$ is free from collisions.
6	Cost Calculation	Compute the cost to reach $q_{new}$ from $q_{start}$ via $q_{nearest}$
7	Rewiring	Check nodes in the vicinity of $q_{new}$ and see if it's more cost-effective to reach them via $q_{new}$ . Update connections accordingly.
8	Goal Check	If $q_{new}$ is close enough to $q_{goal}$ and a direct connection is possible, link them.
9	Completion	Once the goal is reached or after a predefined number of iterations, the algorithm concludes. The optimal path can be traced back from $q_{goal}$ to $q_{start}$ .

### 3. Results and Discussion

#### 3.1. Analysis of clustering algorithms

Considering the parameters in Table 1, camera positions for shooting were generated around the target building in the constructed 3D architectural model. These positions serve as waypoints for the drone during 3D reconstruction. The final result is shown in Fig. 3.

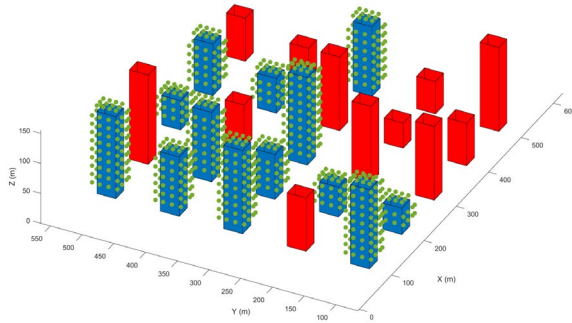


**Fig. 3. 3D representation of buildings.**

Subsequently, the generated waypoints need to be assigned to four drones. To achieve this, the clustering algorithm proposed in this paper, as well as the spectral clustering algorithm used for comparison, were employed to cluster the shooting points. The resulting clusters are depicted in Figs. 4(a) and (b), where points of the same cluster are represented by the same colour.

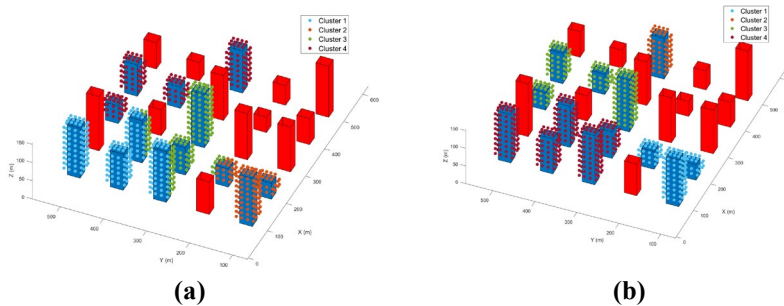


**Fig. 4. Cluster algorithm comparisons (a) Results from the robust and sparse fuzzy K-means clustering algorithm; (b) Outcomes of the spectral clustering algorithm.**

The major difference between the two clustering algorithms discussed in this paper is evident. In the clustering result of the Robust and Sparse Fuzzy K-Means Clustering Algorithm, the position points of a certain building are assigned to two drones, whereas the spectral clustering algorithm assigns all the position points of the entire building to the same drone.



Considering factors such as the spatial location and volume of the target building, it is inevitable that the workload of the four drones will be uneven, with one drone having a disproportionately high workload. The typical flight time of a drone is 20-30 minutes. If it exceeds the battery's working time, it needs to return to change the battery, resulting in a waste of human resources. Therefore, it can be seen that the clustering algorithm proposed in this paper has a greater advantage when applied to the clustering of camera position points for multiple buildings.

### 3.2. Result of path planning

In this section, the F-RRT\* algorithm is employed for path planning on the drone camera capture points generated by two clustering methods. In order to assess the effectiveness of path planning, we have established a cost function based on flight distance and time.

$$J = w_1 \times (D_{\text{horizontal}} + D_{\text{vertical}}) + w_2 \times (T_{\text{horizontal}} + T_{\text{vertical}} + T_{\text{yaw}}) \quad (8)$$

where  $w_1$  and  $w_2$  are weights to balance the effects of distance and time,  $J$  is the total cost,  $D_{\text{horizontal}}$  and  $D_{\text{vertical}}$  is the horizontal and vertical flight distance,  $T_{\text{horizontal}}$  and  $T_{\text{vertical}}$  is the corresponding flight time,  $T_{\text{yaw}}$  is time for the drone to turn. The UAVs flight speed parameters required to calculate the flight time are shown in Table 4.

The path planning of the two clustering methods for the drones is illustrated in Fig. 5. Four drones take off from the safe point in the middle of the map and ascend to a safe altitude before following their respective paths to capture the designated points.

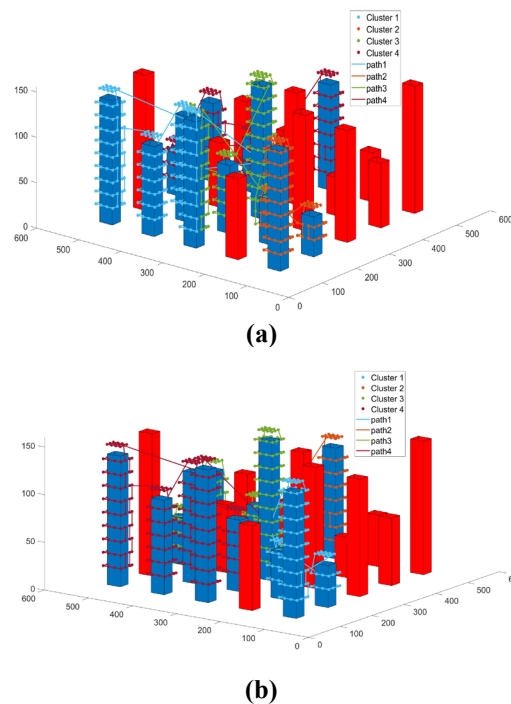


**Fig. 5. Path planning graphs for two clustering algorithms:**  
**(a) Path planning graph for robust and sparse fuzzy K-means clustering**  
**(b) Path planning graph for spectral clustering algorithm.**

**Table 4. Camera shooting point-related parameter.**

Parameter	value	Description
<b>Horizontal flight speed</b>	15/m	Consideration of the distance between drones to avoid flying too close
<b>Vertical Rise Speed</b>	6m/s	Determined by drone speed, camera field of view, and expected image overlap
<b>Vertical descent speed</b>	4m/s	Based on camera focal length, sensor size, and flight altitude
<b>Overlap Measure</b>	12°/s	Optimization of shooting point selection by comparing overlap areas of consecutive images

The simulation graph demonstrates that both clustering algorithms yield optimal drone paths, achieving complete coverage of the target buildings of interest without any collisions. This validates the capability of the F-RRT\* algorithm to generate efficient and safe flight paths in various complex environments. It is worth noting that due to the different assignment of camera capture points by the two clustering algorithms, different cost functions are generated, as shown in Fig. 6.

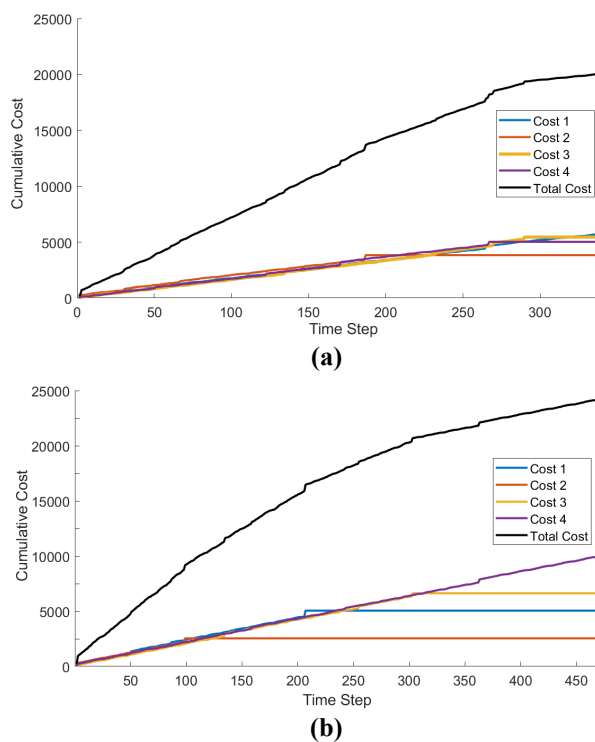


**Fig. 6. Cost function graph path for two clustering algorithms:**  
**(a) Cost function for Robust and sparse fuzzy K-means clustering**  
**(b) Cost function for Spectral clustering algorithm.**

The cost function plots for two clustering scenarios are shown in Fig. 5, with the horizontal axis representing the time taken to complete the path and the vertical axis representing the cost function values. Each plot consists of five curves, which are the cost function curves for four drones individually and their total cost function.

By comparing the images, it is evident that the total cost of the Robust and Sparse Fuzzy K-Means Clustering path is significantly lower than that of the Spectral Clustering algorithm path. Examining the cost function values for the drones in Fig. 6(a), they are notably similar. However, Fig. 6(b) shows a pronounced discrepancy. This discrepancy arises from the uneven distribution of camera points to drones, as determined by different clustering algorithms. Furthermore, the completion time can also be observed from the horizontal axis, with Fig. 6(a) taking 345 timesteps, while Fig. 6(b) takes nearly 470 timesteps. This is the main reason for the significant difference in cost function between the two algorithms.

#### 4. Conclusion

In this research, intricate 3D models of urban structures have been developed, laying the groundwork for subsequent phases. Following the establishment of these models, strategic placement of camera shooting points around the target buildings was executed, adhering to specific predefined parameters. These points were pivotal in facilitating comprehensive capture. Other than that, a comparative study between the Spectral Clustering algorithm and the Robust and Sparse Fuzzy K-Means Clustering Algorithm were discussed, the latter being the focal point of this paper. The analysis revealed that the Robust and Sparse Fuzzy K-Means Clustering Algorithm outperformed its counterpart, adeptly distributing shooting points among four drones. This led to enhanced coverage with reduced redundancy.

Building on this foundation, the F-RRT\* algorithm was applied to determine optimal routes for each UAV. This strategy ensured that the flight paths were not only comprehensive but also tailored to meet each UAV's unique flight capabilities. Our research's strength lies in the amalgamation of potent clustering with sophisticated path planning. The introduction of the Robust and Sparse Fuzzy K-Means Clustering Algorithm stands out, providing a refined strategy for drone task distribution.

Future avenues could delve into real-time trajectory modifications, enabling drones to navigate unexpected challenges or evolving scenarios. Integrating data-driven methodologies might further refine the precision and adaptability of both clustering and navigation phases. To sum up, this work offers a multi-faceted perspective on drone activities within urban landscapes, merging 3D visualization, cutting-edge clustering, and advanced navigation strategies.

#### References

1. Song, L. et al. (2023). The magnitude 6.1 earthquake at the border between China and Kazakhstan on December 1<sup>st</sup>, 2003, and its seismic damage characteristics. *Natural Hazards Research*, 3(4), 632-639.
2. Khanmohammadi, M.; Eshraghi, M.; Sayadi, S.; and Ghafarian, M. (2023). Post-earthquake seismic assessment of residential buildings following Sarpol-e Zahab (Iran) earthquake (Mw7.3) part 1: Damage types and damage states. *Soil Dynamics and Earthquake Engineering*, 173, 108121.
3. Wang, T.; and Gan, V.J. (2023). Automated joint 3D reconstruction and visual inspection for buildings using computer vision and transfer learning. *Automation in Construction*, 149, 104810.

4. Huang, Z.; and Li, D. (2023). A 3D reconstruction method based on one-dimensional galvanometer laser scanning system. *Optics and Lasers in Engineering*, 170, 107787.
5. Creus, P.K.; Sanislav, I.V.; and Dirks, P.H.G.M. (2021). Application of SfM-MVS for mining geology: Capture set-up and automated processing using the Dugald River Zn-Pb-Ag mine as a case study. *Engineering Geology*, 293, 106314.
6. Ye, Y. et al. (2023). A novel triangular stereo model for 3D reconstruction of uniaxial MEMS-based structured light system. *Optics and Lasers in Engineering*, 166, 107596.
7. Phang, S.K.; Chiang, T.H.A.; Happonen, A.; and Chang, M.M.L. (2023). From satellite to UAV-Based remote sensing: A review on precision agriculture. *IEEE Access*, 11, 127057-127076.
8. Wang, F. (2012). Design and construction methodology of an indoor UAV system with embedded vision. *Control and Intelligent Systems*, 40(1), 22.
9. Zheng, X.; Wang, F.; and Li, Z. (2018). A multi-UAV cooperative route planning methodology for 3D fine-resolution building model reconstruction. *ISPRS Journal of Photogrammetry and Remote Sensing*, 146, 483-494.
10. Cui, J.Q. (2016). Search and rescue using multiple drones in post-disaster situation. *Unmanned Systems*, 4(1), 83-96.
11. Yang, C.H.; Tsai, M.H.; Kang, S.C.; and Hung, C.Y. (2018). UAV path planning method for digital terrain model reconstruction-A debris fan example. *Automation in Construction*, 93, 214-230.
12. Kuang, Q.; Wu, J.; Pan, J.; and Zhou, B. (2020). Real-time UAV path planning for autonomous urban scene reconstruction. *Proceedings of the 2020 IEEE International Conference on Robotics and Automation (ICRA)*, Paris, France, 1156-1162.
13. Song, S.; Kim, D.; and Jo, S. (2020). Active 3D modeling via online multi-view stereo. *Proceedings of the 2020 IEEE International Conference on Robotics and Automation (ICRA)*, Paris, France 5284-5291.
14. Nagasawa, R.; Mas, E.; Moya, L.; and Koshimura, S. (2021). Model-based analysis of multi-UAV path planning for surveying postdisaster building damage. *Scientific Reports*, 11(1), 18588.
15. Tai, J.J.; Phang, S.K.; and Wong, F.Y.M. (2022). COAA\* - An optimized obstacle avoidance and navigational algorithm for UAVs operating in partially observable 2D environments. *Unmanned Systems*, 10(2), 159-174.
16. Pang, B.; Hu, X.; Dai, W.; and Low, K.H. (2022). UAV path optimization with an integrated cost assessment model considering third-party risks in metropolitan environments. *Reliability Engineering and System Safety*, 222, 108399.
17. Liu, J. (2023). Deep learning based multi-view stereo matching and 3D scene reconstruction from oblique aerial images. *ISPRS Journal of Photogrammetry and Remote Sensing*, 204, 42-60.
18. Carvajal-Ramírez, F. et al. (2019). Virtual reconstruction of damaged archaeological sites based on unmanned aerial vehicle photogrammetry and 3D modelling. Study case of a southeastern Iberia production area in the bronze age. *Measurement*, 136, 225-236.

19. Phang, S.K.; and Chen, X. (2021). Autonomous tracking and landing on moving ground vehicle with multi-rotor UAV. *Journal of Engineering Science and Technology (JESTEC)*, 16, 2795-2815.
20. Maboudi, M. et al. (2023). A review on viewpoints and path planning for UAV-based 3D reconstruction. *IEEE Journal of Selected Topics in Applied Earth Observations and Remote Sensing*, 16, 5026-5048.
21. Shahid, I.G.; Phang, S.K.; and Chew, W.J. (2023). Fast 3D mapping solution with UAV. *Proceedings of the 18th International Engineering Research Conference 2022 (Eureca 2022)*, *Journal of Physics: Conference Series*, Subang Jaya, Malaysia, 2523(1), 012019.
22. Shi, M.; Zhang, X.; Chen, J.; and Cheng, H. (2023). UAV cluster-assisted task offloading for emergent disaster scenarios. *Applied Sciences*, 13(8), 4724.
23. Ferraro, M.B. (2021). Fuzzy k-Means: history and applications. *Econometrics and Statistics*, 30, 110-123.
24. Zhao, X.; Nie, F.; Wang, R.; and Li, X. (2022). Improving projected fuzzy K-means clustering via robust learning. *Neurocomputing*, 491, 34-43.